Analytical Description of Thermal Control Circuits in Vehicles

Alexander Herzog[✉], Carolina Pelka, and Frank Skorupa

IAV GmbH, Rockwellstraße 16, 38518 Gifhorn, Germany
`dr.alexander.herzog@iav.de`

Abstract. Strict emission standards together with the desire for high efficiency and low fuel consumption necessitate an accurate manipulation of the state variables in the air system of modern combustion engine vehicles. As far as thermal management is concerned, we observe a trend towards on-demand temperature control. The possibilities for such an approach are limited for direct heat exchanging devices, as the efficiency of the thermal transfer is essentially dictated by the vehicle speed. For this reason, indirect heat exchangers are increasingly employed. Such systems allow to implement smart control strategies via appropriate actuators like pumps or valves. This permits to adjust the local temperatures in a wide range, as the efficiency of the heat exchanging device is largely independent of the current driving situation.

On the other hand, robust control strategies usually require the knowledge of the relevant state variables of the system under consideration. Here the desire to minimize the number of sensors follows from economic reasons. However, due to the limited computing power of common automotive CPUs, the possibility to apply numerical methods are also very restricted. From this viewpoint an analytical method to describe the thermal control circuit is desirable. In this paper we outline such an approach. The composition of the cooling fluid may influence the performance of the temperature control system. As the coolant mixture varies for different vehicles and climatic zones, this dependency should be taken into account. Thus, assuming a binary mixture of water and ethylene glycol, we formulate our model for arbitrary volume concentrations.

Our model is based on the method of the so-called dimensionless temperature change, which may be utilized both for single heat-exchangers as well as for entire thermal control circuits. In the latter case, as it turns out, the dimensionless temperature change of the overall system can analytically be traced back to the ones of the individual heat exchangers, which constitute the thermal control circuit. The physical properties of the cooling medium are discussed in detail, where the heat transfer between the working fluid and the cooling medium is described within the frameworks of fluid dynamics. Furthermore, we determine the number of temperature sensors needed for the presented method.

We exemplify the model's validity by means of a thermal control circuit of the indirect charge air cooling device of two different Diesel engine vehicles. Finally, possible generalizations and applications of the model are discussed.

Keywords: Thermal control circuits · Heat exchange · Fluid dynamics

1   Introduction

Recent years have witnessed considerable progress of thermal management systems. Being considered as one of the cornerstones on the route to improved efficiencies and reduced pollutant and greenhouse gas emissions, the developments inter alia span from constructive optimizations of heat exchanging devices and actuators [1, 2] over waste heat recovery [3, 4] to on-demand temperature control strategies [5–8]. The latter topic is essentially facilitated by an increased automation level of the utilized actuators like pumps and valves and bears the prospect not only to realize improvements as far as fuel consumption and tailpipe emissions are concerned, but also in the light of driving comfort and dynamic response. A prominent example for novel concepts in this respect is given e.g. by low temperature charge air cooling, where the working fluid is cooled below ambient temperature [7, 8].

However, alongside the advantages induced by an increased automation level within thermal management systems, they also involve higher complexity, such that the utilized control strategy has to be chosen diligently to provide both performance and stability. Among the various possible approaches, model-based control strategies usually meet these demands, and, in addition offer benefits concerning calibration efforts with the opportunity to minimize the number of cost-intensive sensors. Consequently numerous studies and attempts have been put forward in this direction. For instance in Refs. [9, 10] the coolant flow control for an electric water pump in combination with an intelligent thermostat valve has been investigated. This has been followed by detailed studies on nonlinear control approaches based on the physical model of the thermal management system [11, 12].

Given the aforementioned benefits of model-based control strategies, a severe obstacle for the capability of series production of such algorithms is posed by the limited computing power of common automotive CPUs. This usually requires an analytical description of the systems at hand. In the general case this constitutes a formidable task. As an exception we mention the realization of a model predictive real time controller for an engine cooling system of a truck [13]. Another example for an analytical formulation of a cooling system suited for automotive CPU applications is given by a steady-state model for a simple thermal control circuit, as discussed in Ref. [14]. This model has been formulated for an equimolar mixture of ethylene glycol and water. The validity of the approach has been demonstrated for the indirect charge air cooling device of a Diesel engine vehicle. However, taking the concept of a model-based control strategy seriously and bearing in mind that different vehicle types may contain differing volume concentrations c of ethylene glycol,[1] a model describing the thermal control device should take this dependency explicitly into account. Based on this motivation the present article is concerned with the generalization of the model given in Ref. [14] to arbitrary $c \in [0, 1]$. We give a detailed account of the relevant state variables of the fluids involved in the thermal exchange processes to formulate a closed steady-state model for both the individual heat exchangers as well as the overall temperature control circuit. Our approach is based on the method of the dimensionless temperature change (DTC),

---

[1] The same applies for vehicles in different climatic zones.

which may be utilized for an individual heat exchanger (HE) on the one hand. As it turns out however, an analogous formulation of the overall temperature control circuit under consideration is also possible. We find, that the DTC of the overall system can analytically be traced back to the DTCs of the individual HEs. From this finding we determine the minimum number of temperature signals which have to be provided externally[2] in order to run the presented method. Furthermore, we discuss the physical properties of the cooling medium in detail. Finally, the results drawn from our theoretical approach are discussed in comparison to experimental data obtained from the indirect charge air cooling circuit of two different Diesel engine vehicles.

The paper is organized as follows: In Sect. 2, we discuss the system under consideration and give a brief summary on the method used in Ref. [14] in terms of the present notation. From this, we will see that the closed analytical formulation of the system is induced by the theoretical description of the HEs constituting the thermal control circuit. The approach is based on the representation of the DTCs of the individual HEs by means of the heat capacity flows of the fluids. This task, involving approaches from similitude theory, will be undertaken in Sect. 3. For an automotive application of the model, we have to trace back the heat capacity flows to quantities available to the CPU of the vehicle. This shall be discussed in Sect. 4. Besides well-established formulations for the intake system and the air flow at the front-end of the vehicle, we give a theoretical account on the cooling section. Here the dependency of the cooling fluid properties on the concentration comes into play. The discussion of the experimental setup and details about the calibration of the model are given in Sect. 5. Section 6 gives a comparison of measurements and results obtained from the model. We summarize our findings and give an outline for future research and development perspectives in Sect. 7. The appendix contains details of the cooling fluid properties utilized in Sect. 4 to obtain the coolant heat capacity flow.

2 Formal Description of the Considered Thermal Control System Within the Method of Dimensionless Temperature Change

Apart from the aforementioned steady-state description, throughout the paper the following assumptions concerning the considered system are made:

1. Thermal losses and conversion of internal fluid energies into work as well as phase transitions of the fluids are neglected.
2. The fluids solely occur as single phase.
3. Hoses and pipes are treated as ideal heat insulators, such that lost or gained heat at these elements are not taken into account.

We note, that these assumptions are identical to those made in Ref. [14].

The system under consideration is displayed in Fig. 1, where we have depicted two coupled HEs which are indicated due to the indices 1 and 2. In HE1 two media

---

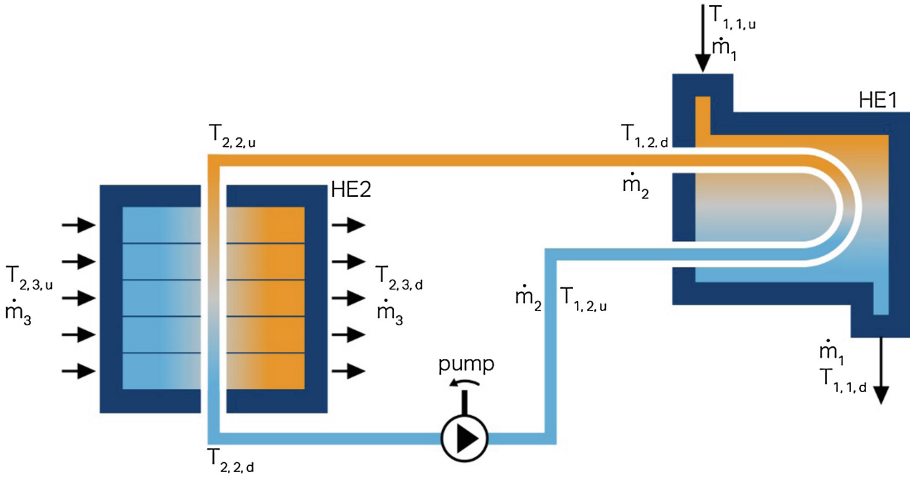[2] E.g. by sensor information or independent models.

Fig. 1. System under consideration: the pump circulates the cooling medium represented by the mass flow $\dot{m}_2$. Thus, enthalpy is extracted from the working fluid mass flow $\dot{m}_1$ in the heat exchanger HE1. The transferred heat decreases the working fluid temperature from $T_{1,1,u}$ to $T_{1,1,d}$ while it heats up the cooling medium from $T_{1,2,u}$ to $T_{1,2,d}$. The dissipated heat is transferred to the ambience in the heat exchanger HE2 where the air flow $\dot{m}_3$ is warmed up from $T_{2,3,u}$ to $T_{2,3,d}$ at the expense of the coolant enthalpy, thus decreasing the cooling medium temperature from $T_{2,2,u}$ to $T_{2,2,d}$.

described by their respective mass flows $\dot{m}_1$ and $\dot{m}_2$ are in thermal contact, where the latter is circulated through the circuit by an electrical pump upstream to HE1. The thermal contact between the fluids given via $\dot{m}_2$ and $\dot{m}_3$ is facilitated in HE2. For the automotive application we have in mind, HE1 represents a specific heat exchanging device at or around the engine compartment (e.g. a charge air or an exhaust gas cooler) and HE2 serves as the cooler at the front-end of the vehicle transferring the dissipated heat to the ambience. Albeit the chosen display of the individual HEs hints at the actual geometries of the respective devices under consideration, the discussion put forward in this section is valid in general and does not depend on the specific construction of the elements. The temperatures at the respective in- and outlets of the HEs are written as $T_{j,l,q}$, where the index $j \in \{1; 2\}$ represents the HE and $l \in \{1; 2; 3\}$ gives the fluid where 1 is attributed to the working fluid, 2 to the coolant, and 3 to the air mass flow induced by the fan and the head wind. Finally, $q \in \{u; d\}$ determines the position respective to the HE j, where u denotes upstream and d downstream to the device in question.

Mind that assumption 3 implies that

$$T_{1,2,\frac{u}{d}} = T_{2,2,\frac{d}{u}}, \tag{1}$$

such that out of the initially eight temperatures, six remain to be determined. In order to simplify the notation, we perform a commensurate shift in the subscripts according to $\{j; l\} = \{1,1; 1,2; 2,3\} \rightarrow \{m\} \{1; 2; 3\}$. Then we may rewrite the temperatures as $T_{m,}$

$_q$, where m now refers to the respective fluid the same way as l, the difference being however, that we have fixed the indexing such that for $m = 2$, the second subscript in the transformed notation refers to the notation of HE1. Thus, in summary, together with Eq. (1), we have $T_{1,q} = T_{1,1,q}$, $T_{2,q} = T_{1,2,q}$, and $T_{3,q} = T_{2,3,q}$. Throughout the paper we assume $T_{1,u} \geq T_{2,u} \geq T_{3,u}$.

In order to model the system represented by Fig. 1, we intend to proceed via the so-called method of DTC [14, 15]. This quantity, referred to as P_i with $i \in \{1; 2\}$, for the HEs shown in Fig. 1, serves as a measure for the efficiency of a heat exchanger. Although the DTC of a HE can be represented both for heating the cooler fluid as well as for cooling the warmer fluid, here we confine ourselves to a formulation where it is given in terms of the latter context. Thus we define it as the ratio of the temperature difference $\Delta T_i = (-1)^{i+1}(T_{i,u} - T_{i,d})$ achieved through the heat exchanging process and the maximum temperature difference being available between the two fluids in thermal contact. For instance, for HE1 this amounts to the temperature difference between the working fluid and the cooling medium upstream to the HE. Within our present notation, we then end up at

$$P_i = (-1)^{i+1} \frac{T_{i,u} - T_{i,d}}{\lambda_i T_{i,u} + (1 - \lambda_i)T_{i,d} - T_{i+1,u}}, \tag{2}$$

where we have defined $\lambda_i = (1 - (-1)^i)/2 \in \{0; 1\}$.

The idea of our approach is to express P_i by means of the heat capacity flows Γ_i and Γ_{i+1} with

$$\Gamma_m = c_{p,m}\dot{m}_m, m \in \{i; i+1\}, \tag{3}$$

i.e.

$$P_i = P_i[\Gamma_i, \Gamma_{i+1}]. \tag{4}$$

Here the specific heat capacity $c_{p,m} = c_{p,m}(T_m)$ is given as a function of the average temperature $T_m := (T_{m,u} + T_{m,d})/2$ at the HE. If furthermore the specific heat capacities $c_{p,m}$ and the mass flows $\dot{m}_m$ can be modelled by analytical means, then, substituting Eq. (4) into Eq. (2), the resulting expression can explicitly be solved for any of the temperatures appearing in Eq. (2), given that the other two temperatures are known.[3] Finally, $T_{i+1,d}$, not appearing in Eq. (2), is determined from the enthalpy balance of the HE, thus reading

$$T_{i+1,d} = T_{i+1,u} - (-1)^i \frac{\Gamma_i}{\Gamma_{i+1}} (T_{i,u} - T_{i,d}). \tag{5}$$

Hence, the knowledge of the DTC by means of the heat capacity flows together with two temperature signals up- or downstream to the HE enables us to calculate the respective other two temperatures at the device [15].

---

[3] E.g. due to values measured by a sensor or given by an independent model.

Generalizing this approach, the overall thermal control circuit depicted in Fig. 1 may effectively be viewed as an overall HE. For this reason we may also define a DTC P_{TCC} corresponding to the entire system as

$$P_{TCC} := \frac{T_{1,u} - T_{1,d}}{T_{1,u} - T_{3,u}}. \tag{6}$$

As it turns out, this expression can be traced back to the DTCs of the HEs constituting the thermal control circuit [14, 15]. This yields

$$P_{TCC} = \frac{\Gamma_2 P_1 P_2}{\Gamma_2 P_2 + \Gamma_1 P_1 (1 - P_2)}. \tag{7}$$

We conclude, that if a representation as given in Eq. (4) can be found for both HEs, we will end up at $P_{TCC} = P_{TCC}[\Gamma_1, \Gamma_2, \Gamma_3]$ with no additional effort at all. Again, from the knowledge of P_{TCC} by means of Eqs. (6) and (7) can be solved for any of the appearing temperatures, given that the other two temperatures are known. The remaining relevant temperatures in the system, not occurring in Eq. (6), may then be determined from local DTC relationships and enthalpy balances.

Summarizing, we conclude, that if we succeed in expressing P_i by means of Eq. (4), and in turn may trace back the heat capacity flows to quantities available to the CPU of the vehicle, the overall cooling system is described in an analytically closed form, given that two temperature signals in the system are known. Therefore, we shall proceed to investigate the DTCs of the individual HEs in more detail in what follows. The description of the heat capacity flows by means of quantities accessible to the CPU shall be postponed to the subsequent section.

3 Models for the Heat Exchangers

3.1 Dimensionless Temperature Changes

In order to model the overall thermal control circuit we have to express the DTCs of HE1 and HE2 by means of the heat capacity flows of the media involved in the heat exchanging processes. The details of the thermal exchange depend on the overall heat transfer coefficient k_i and the heat transfer area A_i of the respective HE. Within the present model these quantities exclusively enter in product form, such that they can be combined as an effective thermal conductibility γ_i as

$$\gamma_i := k_i A_i. \tag{8}$$

Moreover, the explicit form of a HE's DTC depends on its actual topology. Here we assume, the topologies displayed in Fig. 1. Therefore, HE1 exhibits one shell-side with two tube-side passes. The DTC of such a device has been discussed in Refs. [16, 17] and according to our notation reads

$$P_1 = \cfrac{2}{1 + \frac{\Gamma_1}{\Gamma_2} + \sqrt{1 + \left(\frac{\Gamma_1}{\Gamma_2}\right)^2 + \frac{2\Gamma_1}{\Gamma_2}(2\varepsilon - 1)}\coth\left[\cfrac{\gamma_1 \sqrt{1 + \left(\frac{\Gamma_1}{\Gamma_2}\right)^2 + \frac{2\Gamma_1}{\Gamma_2}(2\varepsilon - 1)}}{2\Gamma_1}\right]}, \qquad (9)$$

where ε takes account of differences between the two passes, due to distinctions in the effective heat transfer areas and heat transfer coefficients [15].

The topology of HE2 shown in Fig. 1 resembles a cross-flow HE where the fluids are laterally mixed on both sides. For such a device the DTC reads [18]

$$P_2 = 1 - \exp\left[\frac{\Gamma_3}{\Gamma_2}\left(e^{-\frac{\gamma_2}{\Gamma_3}} - 1\right)\right]. \qquad (10)$$

Thus, apart from the heat capacity flows, the dependency of P_i on the effective thermal conductibility has to be taken into account for both HEs. As we will see however, γ_i can be traced back to Γ_i and Γ_{i+1}, thus

$$\gamma_i = \gamma_i[\Gamma_i, \Gamma_{i+1}]. \qquad (11)$$

This shall be discussed in the following subsection.

3.2 Thermal Conductibility

From the theory of heat transfer it is known that the overall thermal resistivity, being the reciprocal value of the respective thermal conductibility, is given by the sum of the individual thermal resistivities of the materials facilitating the thermal contact. Thus, for $i \in \{1, 2\}$ we have

$$\frac{1}{\gamma_i} = \frac{1}{\alpha_i A_i} + \frac{\delta}{\lambda A_M} + \frac{1}{\alpha_{i+1} A_{i+1}}, \qquad (12)$$

The heat transfer coefficient of the fluid $m \in \{i; i+1\}$ transmitted through the area A_m is given by α_m. The material properties of the HE have been taken account of by the thickness δ, the area A_M and the thermal conductivity λ. Assuming $A_i = A_{i+1} = A_M$ throughout what follows, a crude estimation of typical heat transfer coefficients reveals that the thermal resistivity of both fluids does exceed the one of the HE material by at least two orders of magnitude. Therefore, it seems permissible to neglect this term. Furthermore, as is well-known, the heat transfer coefficient α_m can be reformulated by means of the respective Nusselt number Nu_m via

$$\alpha_m = \frac{\lambda_m Nu_m}{L}, \qquad (13)$$

where $\lambda_m = \lambda_m(T_m)$ describes the heat conductivity of the fluid m and L is a characteristic length of the device.

On the other hand the Nusselt number of a fluid can be expressed by the corresponding Reynolds and Prandtl number. For our present purposes we write the Reynolds number as

$$\mathrm{Re}_m = \frac{L}{A_m c_{p,m} \eta_m} \Gamma_m, \tag{14}$$

with the dynamic viscosity $\eta_m = \eta_m(T_m)$. The Prandtl number is given by

$$\mathrm{Pr}_m = \frac{\eta_m c_{p,m}}{\lambda_m}. \tag{15}$$

In the present context, the heat conductivity λ_m, the specific heat capacity $c_{p,m}$ and the dynamic viscosity η_m can be regarded as mere functions of the average temperature T_m. Thus, the heat transfer coefficient can, combining Eqs. (13)–(15), be separated into a product of a function of the average temperature $\widetilde{g}(T_m)$ and a function of the heat capacity flow $f(\Gamma_m)$.

For thermal exchange problems it is quite common in automotive applications to assume a power-law relation between Nu_m, Re_m and Pr_m [19]. From this the heat transfer coefficient α_m may be cast into the form

$$\alpha_m = \Gamma_m^{n_m} \widetilde{g}(T_m). \tag{16}$$

where the function $\widetilde{g}(T_m)$ does only weakly depend on the average temperature and may thus be approximated by the constant g_m. Furthermore, we assume a universal exponent n_m for the two media which are in thermal contact through the HE under consideration. Taking this into account we finally end up at a three parameter theory for the thermal conductibility of the HE, which has to be fitted to given experimental data. We stress that the thermal conductibility is a quantity which is essentially induced by convection. Therefore γ_i turns out to be a strictly increasing, yet saturating function of Γ_i and Γ_{i+1}.

Once the aforementioned three parameters are determined, the DTC of each HE is solely given by means of the heat capacity flows of the respective fluids (c.f. Eqs. (9) and (10)). In the next section, we will investigate these quantities in more detail.

4   Model for the Heat Capacity Flows

The heat capacity flow of the fluid m is given by Eq. (3). Thus, for each medium we have to determine both the specific heat capacity and the respective mass flow.

4.1   Heat Capacity Flow for the Intake Air and the Head Wind

The mass flow $\dot{m}_1$ of the working fluid is given by the sum of the mass flow of fresh air $\dot{m}_{1,\mathrm{F}}$ and the mass flow of recirculated exhaust gas $\dot{m}_{1,\mathrm{EGR}}$ streaming through HE1.

Usually the mass flow of fresh air is measured by an airflow sensor. The recirculated mass flow can be modelled by a one-dimensional mass flow balance [20]. As far as the head wind is concerned, the corresponding mass flow can be determined as a function of the vehicle velocity and the rotational speed of the fan at the front-end. A correction due to the state variables of the ambience is taken into account.

We model the specific heat capacity of air in the relevant temperature regime according to

$$c_{p,A} = \begin{cases} c_{p,A,0} & \forall T_A < 293,15K \\ c_{p,A,1(T_A)} & \forall T_A \geq 293,15K' \end{cases} \tag{17}$$

where $c_{p,A,0}$ is a constant and $c_{p,A,1}(T_A)$ is given by a second order polynomial of the local air temperature T_A. This expression is used both for the determination of the specific heat capacity of the head wind and the fresh air share in the working fluid. For the latter, however, we also have to take into account that the specific heat capacity of the recirculated exhaust gas may differ significantly from $c_{p,A}$. To this end, we formulate the specific heat capacity $c_{p,1}$ of the gas flowing through HE1 on the footing of energy conservation

$$c_{p,1} = c_{p,A}(1 - r_{EGR}) + r_{EGR}c_{p,EGR}, \tag{18}$$

where the recirculated exhaust gas rate $r_{EGR} = \dot{m}_{1,EGR}/\dot{m}_1$ has been used.

In the present context we assume the exhaust gas to consist of air, water, and carbon dioxide. The specific heat capacity of the recirculated exhaust gas may then be determined in analogy to Eq. (18) where we assume the water- and carbon dioxide-rates to be constant within the exhaust gas. They are fitted to vehicle measurements.

The temperature dependence of the isobaric specific heat capacity of carbon dioxide is approximated to linear order in the given temperature range. The specific heat capacity of liquid water is discussed in the appendix, whereas for water vapor a constant value may be assumed.

Thus the heat capacity flow of the intake gas is determined.

4.2 Heat Capacity Flow for the Coolant

We model the coolant mass flow through a pipe segment in the cooling circuit by means of the Hagen-Poiseuille equation [21]:

$$\dot{m}_2\left(c, T_{2,u}, r\right) = C\varrho_2\left(c, T_{2,u}\right) \frac{\Delta p\left(c, T_{2,u}, r\right)}{\eta_2\left(c, T_{2,u}\right)}. \tag{19}$$

Both the dynamic viscosity η_2 as well as the density ϱ_2 of the coolant exhibit a dependence on volume concentration c and temperature $T_{2,u}$.[4] The pressure drop Δp in the considered pipe segment does also depend on these quantities. Here, in addition, the rotational speed of the pump n_P comes into play. We define $r := n_P/n_{P,max}$ as the rotational speed normalized to the respective maximum value $n_{P,max}$. Finally, C takes account of the geometry of the segment.

For a discussion of the dynamic viscosity and the density of the fluid, we refer the reader to the appendix. Apart from this, we have to model the pressure drop in the pipe segment by means of $x, T_{2,u}$, and r. For an incompressible fluid we find

$$\Delta p\big(c, T_{2,u}, r\big) = \varrho\big(c, T_{2,u}\big)a(c, r). \tag{20}$$

Here the acceleration a induced by the pump is assumed to depend on c and r. An explicit temperature dependence is excluded as can be justified by means of vehicle measurements. We write $a(c, r) = a_\xi(c)a_\zeta(r)$ where we put $a_\xi(r) = r^2 + \xi r^3$ and $a_\zeta(c) = 1 + \zeta_1 c + \zeta_2 c^2$. The parameters ξ, ζ_1, and ζ_2 are fitted to vehicle measurements.

Being a generic property of the cooling medium the specific heat capacity of the coolant is discussed in the appendix. Thus the heat capacity flow of the cooling medium is determined as a function of $c, T_{2,u}$, and r.

5 Experimental Details and Calibration

The predictions of our model shall be compared to experimental data obtained from two charged Diesel engine vehicles referred to as V1 and V2 henceforth. Both test carriers have a displacement of two liters and the rated power outputs are given by 140 and 110 kW respectively. The system under consideration consists of the thermal control circuit of the indirect charge air cooling device of V1 and V2.

All parameters required to describe the properties of the cooling mixture, as discussed in the appendix, have been calibrated on the basis of the respective data sheets of the cooling medium. Here we briefly summarize our findings in this respect. The density of water and ethylene glycol can be modelled by a three and a two-parameter theory respectively. By the conservation of mass the interpolated density for the coolant mixture is then given by a mere linear combination with respect to the volume concentration of the densities of the respective pure agents. The dynamic viscosity is given by a three-parameter theory for the respective pure fluids and the interpolation can be taken account of by a two-parameter model. Contrary to this, the interpolation for the specific heat capacity of the coolant mixture is determined from the conservation of energy and does hence not require any free parameters. However, in order to give a satisfying account of this quantity, for the pure components, the PDDS equation, taking the lowest four orders into account, is used [15]. Finally, the heat conductivity of water can be approximated by a second order polynomial, whereas this property can be

---

[4] We have chosen a pipe segment in the inlet flow because temperature effects are much more crucial here due to the exponential temperature behavior of the viscosity (c.f. the appendix).

captured by a linear approximation for ethylene glycol. The interpolation for the mixture is well-described by a two-parameter interpolation. In total we thus utilize mutually independent models for the properties of the pure agents with up to four parameters. The interpolation for the coolant mixture, if not restricted by mass- or energy conservation may then be obtained by independent two-parameter models.

In order to calibrate our mass flow model, a measuring device, combining a volume flow and a temperature sensor, has been installed in the cooling circuits. The parameters are fitted to vehicle measurements where the rotational speed of the pump is varied for different volume concentrations under numerous ambient conditions. As suggested by the model, we do not observe any temperature dependence for a (c.f. Eq. (20)). Thus, together with the fitting process for the specific heat capacity of the working fluid outlined in Subsect. 4.1, the heat capacity flows of all media involved within the model are at our disposal.

Finally, the calibration of the models for the individual heat exchangers can be executed. To this end the test carriers were equipped with temperature sensors up- and downstream to the respective charge air coolers for the two media in thermal contact. A further temperature sensor has been installed upstream to the cooler at the front-end on the head wind side. In a multi-stage fitting procedure, taking both the DTCs of the individual HEs as well as the overall DTC of the integral cooling device into account, the three free parameters of each $\gamma_i, i \in \{1; 2\}$, introduced in Subsect. 3.2, were determined. This final step completes the calibration of the model.

6   Results

In this section we compare the results predicted from the calibrated model with vehicle measurements. Within this report the DTC has served as the central quantity when discussing individual HEs and the overall thermal control system. The quality of the described method depends crucially on the possibility to represent the individual DTCs (c.f. Eq. (2)) by means of the respective heat capacity flows as given by Eqs. (9) and (10). In Figs. 2 and 3 the DTCs of the charge air coolers of the investigated test vehicles are exemplified. For V1 a comparison between experiment and theory is displayed in Fig. 2. The surface illustrates a connected envelope of our model for P_1 as a function of the normalized heat capacity flows $\Gamma_1/\Gamma_{1,max}$ for the intake gas and $\Gamma_2/\Gamma_{2,max}$ for the cooling medium. Here $\Gamma_{m,max}$ gives the maximum value observed for the heat capacity flow of the fluid m. The model is to be compared to the respective measure points shown in the plot, where test series were recorded for pure water, pure ethylene glycol and a mixture with $c = 0.6$. Overall we find good agreement between theory and experiment. As predicted by the model, P_1 does not explicitly depend on the volume concentration. Instead this dependency comes into play implicitly, as Γ_2 is a function of c. Note in particular the tendency of an increased cooling fluid heat capacity flow with decreasing volume concentration. This is of course essentially induced both by the lower viscosity resulting from the smaller content of ethylene glycol and the high specific heat capacity of water. We furthermore observe that the DTC of the charge air cooler is a monotonically increasing function of Γ_2. The physical picture behind this finding is intuitively clear: The bigger the heat capacity flow of the coolant,
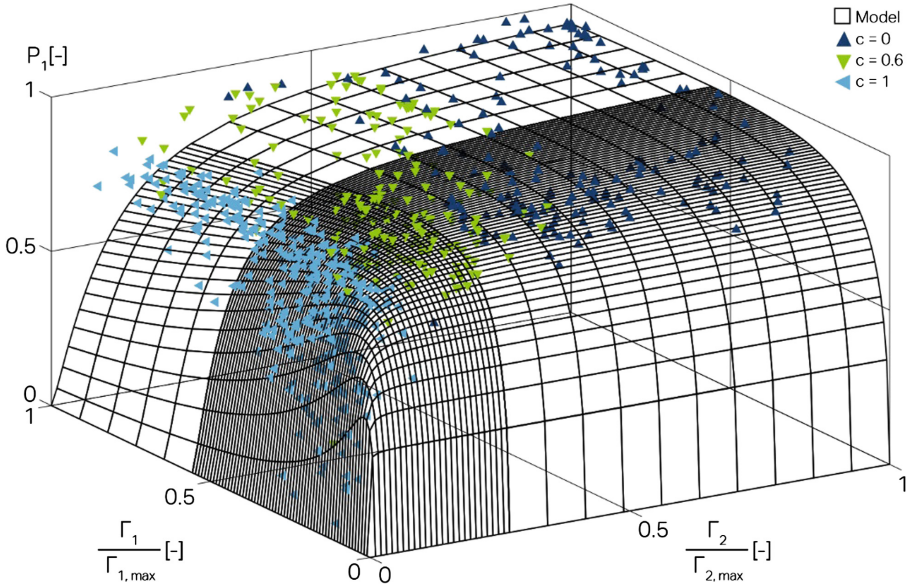
Fig. 2. Dimensionless temperature change as a function of the normalized heat capacity flows of intake air and cooling fluid for the charge air cooler of the Diesel engine vehicle with 140 kW rated power output. A comparison between our model (surface) and experimental data (symbols) for the pure agents as a well as for a mixture with 60 % volume concentration in ethylene glycol is displayed.

be it due to an increased mass flow or specific heat capacity, the higher the performance of the heat exchanging process. Due to the pronounced nonlinearity of P_1, the gradient along an increasing heat capacity flow is very steep for small Γ_2 and falls off rapidly for $\Gamma_2/\Gamma_{2,max} \gg \Gamma_1/\Gamma_{1,max}$ such that the DTC saturates in this regime.

Applying the simple picture utilized to explain the tendency of increasing P_1 with increasing Γ_2 suggests that an inverse behavior should be observed along the heat capacity flow of the intake air, i.e. the DTC should diminish with growing Γ_1. This indeed is observed for sufficiently high values of Γ_1. However, we find, that along Γ_1 the DTC of the charge air cooler does not monotonically decrease. Instead we have

$$\lim_{\Gamma_1 \to 0} P_1(\Gamma_1, \Gamma_2) = 0. \tag{21}$$

Consequently for $\Gamma_1 \ll \Gamma_{1,max}$ we find

$$\frac{\partial P_1}{\partial \Gamma_1} > 0. \tag{22}$$

This is due to the fact that the effective heat conductibility γ_1 monotonically increases with increasing heat capacity flow, as the heat transfer processes are facilitated by convective means (c.f. Sect. 3.2). Therefore, starting from small Γ_1, we find a
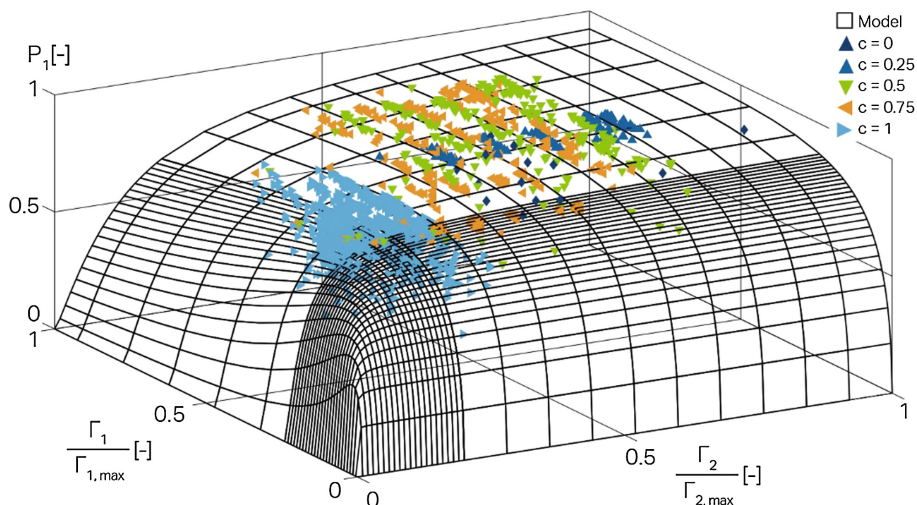
Fig. 3. Dimensionless temperature change as a function of the normalized heat capacity flows of intake air and cooling fluid for the charge air cooler of the Diesel engine vehicle with 110 kW rated power output. A comparison between our model (surface) and experimental data (symbols) for various volume concentrations is displayed.

steep positive slope in the DTC of the HE. Along Γ_1 the DTC runs through a maximum for fixed Γ_2 from which the aforementioned decrease of P_1 for increasing Γ_1 is observed. The maximum occurs in the region, where the thermal conductibility is close to saturation, i.e. for values where an increase in Γ_1 does not lead to a significant increase in γ_1 which could compensate the greater amount of heat to be transferred away from the intake air.

Turning to V2 (c.f. Fig. 3) all these findings are confirmed. The experimental values displayed by the measure points for various volume concentrations as indicated in the plot are in good accordance with the theoretical predictions, again shown as a connected envelope.

In Fig. 4, the analytically closed model for the DTC of the integral cooling system (c.f. Eq. (7)) of V1 is compared to the respective measure points. Here merely points which correspond to a given value of the heat capacity flow of the head wind allow for a significant comparison. The chosen data corresponds to a vehicle velocity of 120.5 ± 0.5 km/h with an inactive fan. The experimental results are to be compared with the surface shown in Fig. 4. As for the individual HEs the DTC of the overall cooling circuit is well-described within our model. We have checked that this is also true for other values of the head wind heat capacity flow.

Along increasing Γ_2 we find that the DTC of the thermal system is monotonically increasing, where a saturation effect is observed for sufficiently high Γ_2. Unlike for the individual HE such a behavior is not necessarily fulfilled for the overall system. As Γ_2
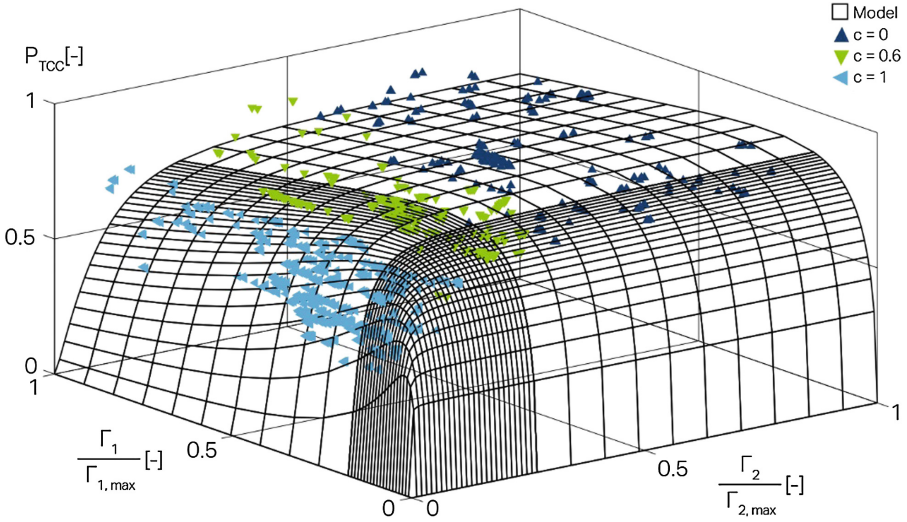
Fig. 4. Dimensionless temperature change for the overall thermal control system as a function of the normalized heat capacity flows of intake air and cooling fluid for the Diesel engine vehicle with 140 kW rated power output. The displayed data corresponds to a constant heat capacity flow of the head wind at a vehicle speed of 120.5 ± 0.5 km/h with inactive fan. A comparison between our model (surface) and experimental data (symbols) for various volume concentrations is displayed.

has respectively opposing impacts on P_1 and P_2,[5] there may exist operating points, with $\partial P_{TCC}/\partial \Gamma_2 < 0$. However, such a behavior has not been observed for the two test vehicles under consideration.

Contrarily, along the intake air heat capacity flow P_{TCC} runs through a maximum value for any fixed Γ_2 and falls of towards higher Γ_1. This behavior clearly resembles our findings for P_1. As P_2 does not depend on the heat capacity flow of the intake air, this effect already studied for the DTC of the charge air cooler remains pronounced for the overall system. Finally, we want to stress, that P_{TCC} increases with increasing Γ_3. This is of course due to the fact, that P_2 turns out to increase with increasing Γ_3. This effect is clearly attributed to the circumstance, that the heat transfer from the cooling medium to the ambience necessitates a sufficiently high heat capacity flow due to the head wind.

Figure 5 contains a representation of the DTC of the overall charge air cooling system for V2. Here Γ_3 corresponds to a vehicle velocity of 98 ± 2 km/h with an inactive fan. As for the other test car we find good agreement between the measured data (symbols) and the surface calculated from the model. The findings discussed for Fig. 4 are reproduced for this vehicle.

For both test cars we find the tendency that a decreased volume concentration c leads to an increased coolant heat capacity flow due to viscosity and specific heat capacity effects. This results in slight but significant differences in the absolute values of the DTC for the thermal control circuit. These slight differences may however have a

---

[5] I.e. P_1 increases with increasing Γ_2, whereas P_2 decreases in that case.
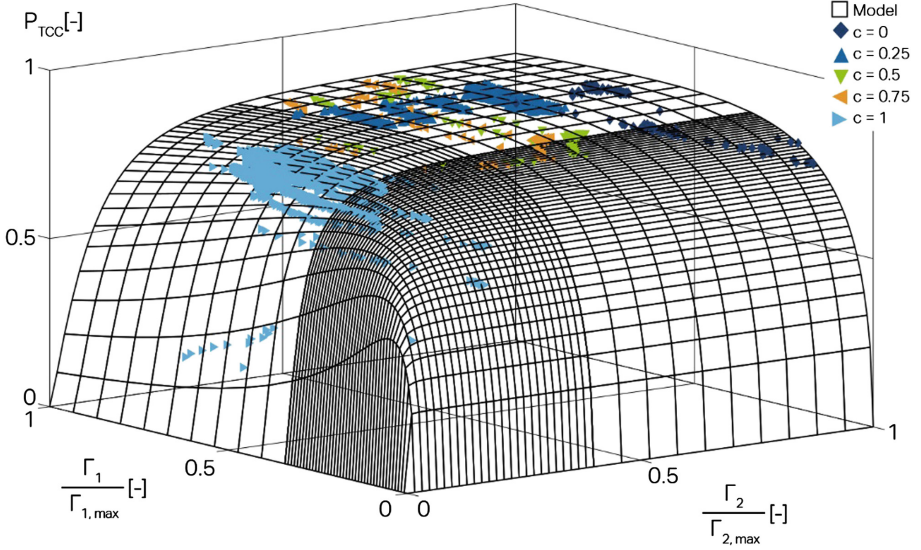
Fig. 5. Dimensionless temperature change for the overall thermal control system as a function of the normalized heat capacity flows of intake air and cooling fluid for the Diesel engine vehicle with 110 kW rated power output. The displayed data corresponds to a constant heat capacity flow of the head wind at a vehicle speed of 98 ± 2 km/h with inactive fan. A comparison between our model (surface) and experimental data (symbols) for various volume concentrations of ethylene glycol is displayed.

distinct effect on the respective fluid temperatures as P_{TCC} occurs in combination with large absolute temperatures or temperature differences. Moreover, this has an impact on the model for Γ_2 and underlines the importance to take the adequate volume concentration into account, when model-based applications like diagnostics and control are utilized for series production.

Finally we want to apply the presented method to model the temperature downstream to the charge air cooler of the two vehicles. To this end we rewrite Eq. (6) as

$$T_{1,d} = T_{1,u} - P_{TCC}[\Gamma_1, \Gamma_2, \Gamma_3](T_{1,u} - T_{3,u}), \tag{23}$$

where $T_{1,u}$ and $T_{3,u}$ are provided by sensor signals. In Fig. 6 representative results from this approach (solid lines) are compared with experimental data (dotted lines) drawn from measurements performed for V1. Here the volume concentrations $c = 0$, $c = 0.6$, and $c = 1$ have been investigated (c.f. Fig. 6(a), (b) and (c) respectively). For confidential reasons a constant reference temperature $T_{1,d,\text{Ref}}$ has been subtracted from the absolute value of $T_{1,d}$. The left inset shown in Fig. 6(a) displays the corresponding signal for the temperature upstream to the charge air cooler also shifted by a constant reference temperature $T_{1,u,\text{Ref}}$. The normalized heat capacity flow of the intake air is depicted in the right inset of Fig. 6(a). Both insets underline that the measurements mostly resemble dynamical driving situations. Albeit the presented model is based on a

steady-state formulation, the results drawn from the model do agree well with the experimental data for $c = 0$. The same may be said for $c = 0.6$ and $c = 1$ displayed in Figs. 6(b) and (c) respectively. Here also experimental data of the shifted intake air temperature downstream to the charge air cooler is compared to the corresponding values obtained from our model. These measurements also do represent dynamical driving situations. Taking all measurements into account, we find that the mean absolute deviation

$$\delta T_{1,d} := \frac{\sum_{q=1}^{q_{max}} \left| T_{1,d,mod} - T_{1,d,meas} \right|}{q_{max}}$$

between model and experiment is given by 4.17K for this vehicle. Here we have averaged the absolute values of the deviation between theory and experiment, respectively given by $T_{1,d,mod}$ and $T_{1,d,meas}$ over the overall number q_{max} of recorded time slots.

For V2 the shifted charge air temperature as given by our model is compared to experimental data in Fig. 7. The corresponding volume concentrations are $c = 0$ (c.f. Fig. 7(a)), $c = 0.5$ (c.f. Fig. 7(b)), and $c = 1$ (c.f. Fig. 7(c)). Again for $c = 0$ the transient nature of the underlying driving situation is clearly displayed by the supplemented insets. Summarizing, we find that the predictions from our model correlate well with the measurement data, albeit the accuracy is a little reduced in comparison to V1. This is also reflected in the mean absolute deviation for this vehicle which is given by $\delta T_{1,d} = 4.7$K. However, these deviations should be compared to those obtained in Ref. [14], where a mean absolute deviation of 5K was given for a test vehicle with a strictly equimolar mixture of ethylene glycol and water. We stress that restricting the range of application of the volume concentration allows a more accurate calibration of the model parameters. From this a further reduction of the mean absolute deviation between measurement and model data would result. Taking into account that the presented model is sufficiently simple to be run on an automotive CPU, the approach exhibits an overall satisfying accuracy. Finally, we like to point out, that the model interpolates smoothly as a function of c.

Having determined $T_{1,d}$, the coolant temperature up- and downstream to the charge air cooler can be obtained by means of the DTC of the individual HEs and local enthalpy balances. Figure 8 shows a representative comparison between the model values (solid line) of the coolant temperature and corresponding experimental data (dotted line). In Fig. 8(a) the cooling fluid temperature $T_{2,u}$ upstream to the charge air cooler is displayed, where again a constant reference temperature $T_{2,u,Ref}$ has been subtracted from both data sets. Due to error propagation, the accuracy of the modeled coolant temperature is a little reduced in comparison to $T_{1,d}$. However, the model may still serve as a quantitative estimation for the coolant temperature upstream to the charge air cooler. Here the test vehicle with 110 kW rated power output has been used with a volume concentration of $c = 0.25$. Again the measurement resembles dynamic driving situations. The corresponding measurement for the coolant temperature downstream to the charge air cooler is depicted in Fig. 8(b). We observe good agreement between theory and experiment, such that the model for instance may be utilized to detect critical temperatures in the charge air cooler outlet.
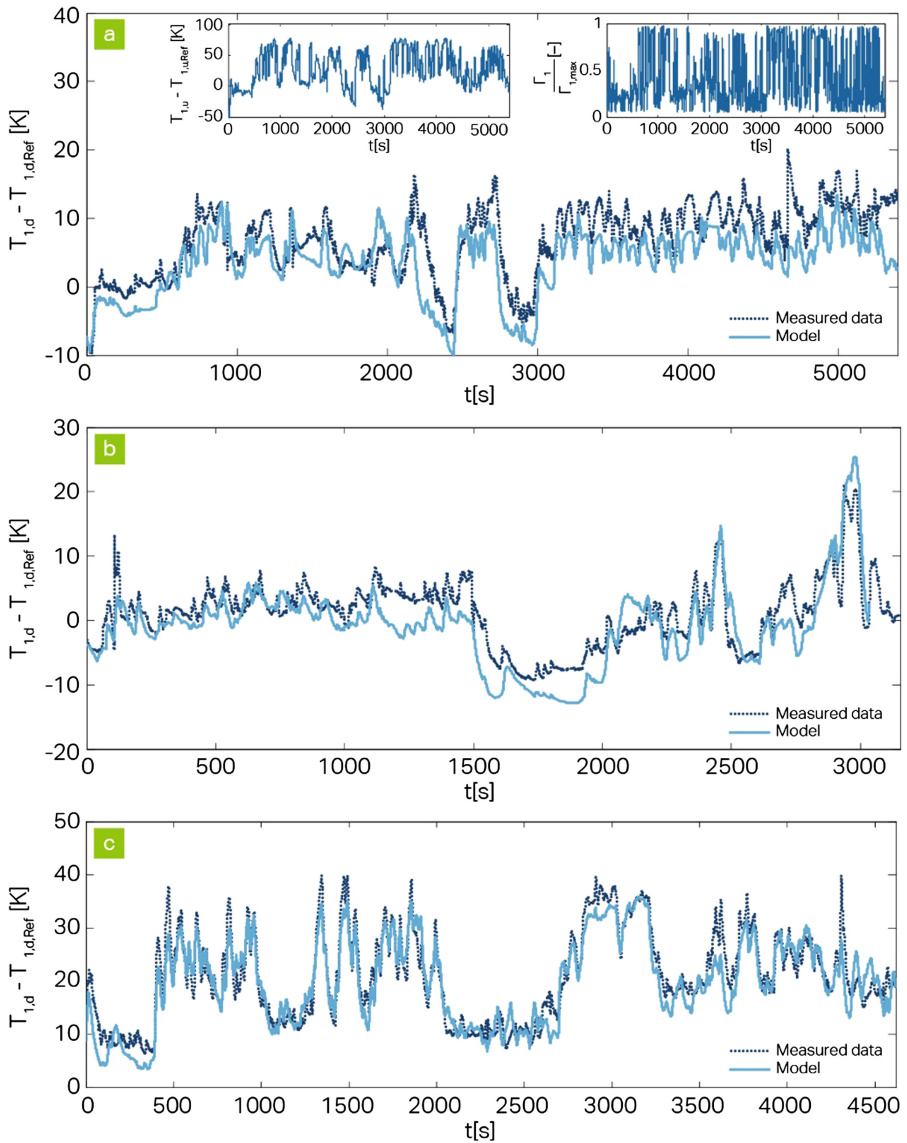
Fig. 6. Comparison between experimental data (dotted line) and predictions of the calibrated model (solid line) for several volume concentrations of ethylene glycol. The intake air temperature downstream to the charge air cooler of the vehicle with lower rated power output is shown. (a) Pure water: In order to illustrate the transient nature of the driving situations, the left inset displays the respective intake air temperature upstream to the charge air cooler. In the right inset the corresponding intake air heat capacity flow is depicted. (b) 60 % volume concentration of ethylene glycol. (c) Pure ethylene glycol
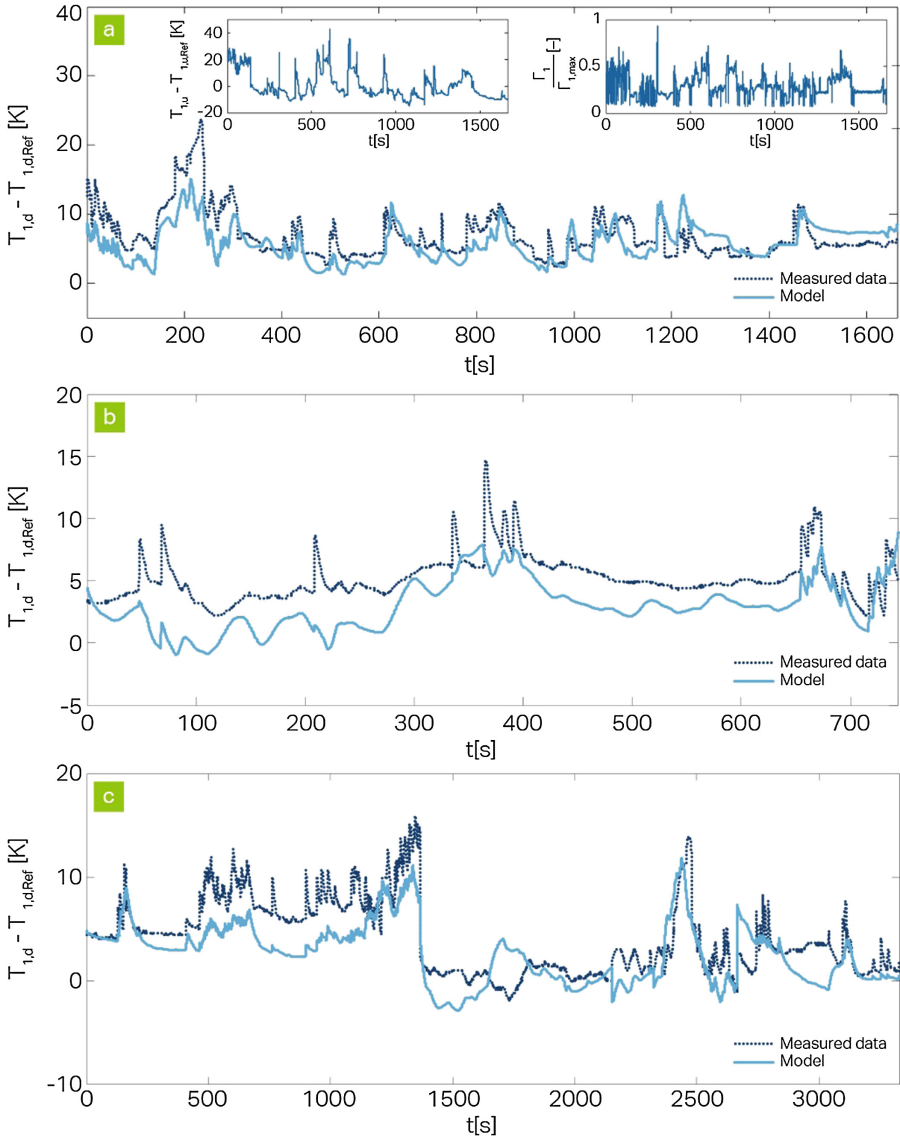
Fig. 7. Comparison between experimental data (dotted line) and predictions of the calibrated model (solid line) for several volume concentrations of ethylene glycol. The intake air temperature downstream to the charge air cooler of the vehicle with 110 kW rated power output is shown. (a) Pure water: In order to illustrate the transient nature of the driving situation the left inset displays the respective intake air temperature upstream to the charge air cooler. In the right inset the corresponding intake air heat capacity flow is depicted. (b) 50 % volume concentration of ethylene glycol. (c) Pure ethylene glycol.
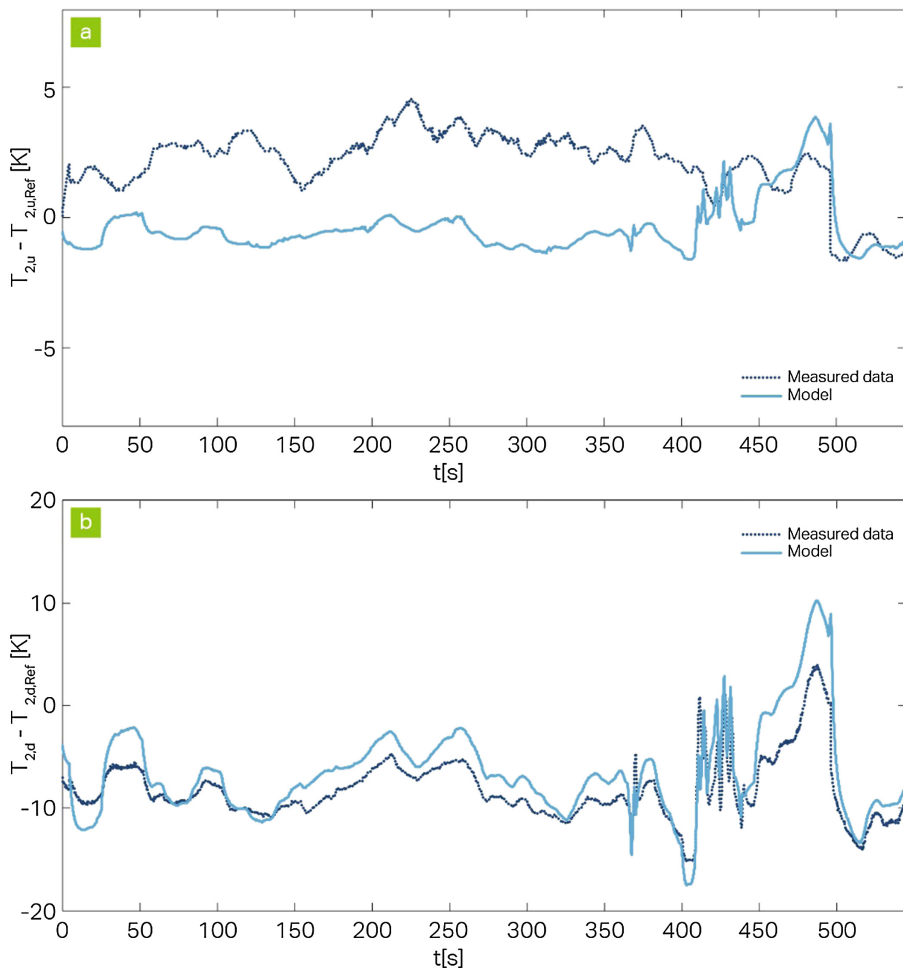
Fig. 8. Comparison between theoretical (solid line) and experimental (dotted line) values for the cooling fluid temperature in the vehicle with 110 kW rated power output. Here, a mixture with an ethylene glycol volume concentration of 25 % has been used. (a) Coolant temperature upstream to the charge air cooler. (b) Coolant temperature downstream to the charge air cooler.

7   Summary and Outlook

In this paper we have investigated a simple temperature control circuit which consists of a heat exchanger in the air intake or exhaust gas system of a vehicle with a combustion engine. We have argued that the growing automation level of the actuating elements in thermal management systems bears good prospects to realize advantages concerning tailpipe emissions and fuel consumption. Driving comfort and transient response may also be improved by thermal on-demand control strategies. Among the latter, model-based concepts offer advantages as far as control stability and calibration

efforts are concerned. In this spirit, formulating the thermal control circuit by analytical means, the volume concentration of ethylene glycol should be treated as a model parameter, as different vehicle types and vehicles in different climatic zones exhibit different cooling fluid mixtures. A theoretical approach taking this dependency explicitly into account has been discussed in this paper, where the full range between pure water and pure ethylene glycol has been covered. The model is based on the method of dimensionless temperature change. This quantity can be defined both for individual heat exchangers as well as for the overall temperature control circuit and may be interpreted as the efficiency of the heat exchanging device under consideration. The dimensionless temperature change of the overall circuit can be traced back to the ones of the individual heat exchangers (c.f. Eq. (7)). Thus, if the dimensionless temperature changes of the individual heat exchangers can be expressed by quantities available to the CPU of the vehicle, the considered overall temperature control system may by described by analytical means without any additional calibration effort at all. The representation of the individual dimensionless temperature changes by means of the fluid heat capacity flows was discussed on the basis of heat transfer and similitude theory. Provided that two temperature signals of the overall system are known from sensor information or from an independent model, the remaining four non-trivial temperatures can be determined with the presented method.

The fluid properties were described in the framework of well-established phenomenological models. Here the dependency of the volume concentration of ethylene glycol in the coolant mixture comes explicitly into play. In general, the cooling medium properties are discussed in terms of the pure agents (i.e. water and ethylene glycol). For an arbitrary volume concentration interpolation models are used. In particular, we find that the individual dimensionless temperature changes do not explicitly depend on the volume concentration. Instead, this dependency merely enters implicitly by means of the cooling fluid properties. To our satisfaction, this theoretical prediction is confirmed by experiment.

Summarizing, the presented approach consists of various mutually independent models for the fluid properties, the thermal conductibilities, and the dimensionless temperature changes of the individual heat exchangers. Each model is expressed by means of elementary functions such that the suggested approach is suited for automotive CPU applications.

We have applied our model to the indirect charge air cooling devices of two Diesel engine vehicles with different rated power outputs. Using the ambient temperature and the intake air temperature upstream to the charge air cooler as reference information, we have utilized the dimensionless temperature change of the overall temperature control circuit to determine the charge air temperature. A comparison to experimental data exhibits good accordance between model and measurement. In particular, not only the steady-state but also the transient behavior of the thermal system is captured within our model. For both test vehicles, we have exemplified the quality of our model for three distinct volume concentrations of ethylene glycol. Overall we find a mean absolute deviation between measurement and model of 4.17 and 4.7K for the charge air temperature of the higher and lower rated power output vehicle respectively. We have checked, that the model interpolates correctly between the individual ethylene glycol volume concentrations. We stress that the model has been calibrated for the whole

range of volume concentration between zero and one. Limiting this region during the calibration process naturally restricts the applicability of the model. However, this restriction on the other hand comes with a benefit regarding model accuracy.

Moreover, utilizing the dimensionless temperature changes for the individual heat exchangers as well as enthalpy balances, the coolant temperature up- and downstream to the respective charge air cooler were determined. A comparison between theory and experiment reveals satisfying agreement. For instance, the model may be applied to detect critical temperatures in the cooling circuit.

The presented model has been motivated on the footing of model-based automotive applications such as control or diagnosis with the application of heat exchanging devices in the intake air or exhaust gas system. The approach may be utilized to minimize the number of temperature sensors within a temperature control device resembling the system discussed in this report. However, the overall temperature control systems of vehicle engines are more complex than the simple cooling circuit we have addressed here. Therefore, a generalization of the approach outlined in this paper is highly desirable. Of course with an increased complexity of the system not only the theoretical description will be more involved. Also the treatment of the temperature control problem is much more demanding in that case, as different components may have different and even mutually excluding requirements. Also in this case, model-based decision making and control may help to further reduce pollutant emissions or to improve the efficiency of combustion engines.

A Appendix: Properties of the Coolant Mixture

Throughout the paper, the importance of the volume concentration c of ethylene glycol has been stressed. In this appendix we want to give a detailed account on the properties of the mixture as a function of c. To this end we discuss the respective properties of the pure substances respectively in a first step.[6] The resulting models are then interpolated as a function of the volume concentration of ethylene glycol c. Throughout this appendix our models for the fluid properties are compared to experimental data given in a data sheet of the coolant producer.

Note that strictly speaking an additive rule for the individual volumes does not apply. However, effects stemming from this circumstance turn out to be negligible and are therefore ignored within our investigations.

In general, the interpolation used to describe a fluid property $y(T_{2,q})$ by means of the respective properties of the pure components $y_{C_2H_6O_2}(T_{2,q})$ and $y_{H_2O}(T_{2,q})$ is realized by the interpolating functions $h_y(c, T_{2,q})$ and $\overline{h}_y(c, T_{2,q})$ such that

$$y(T_{2,q}) = h_y(c, T_{2,q})y_{C_2H_6O_2}(T_{2,q}) + \overline{h}_y(c, T_{2,q})y_{H_2O}(T_{2,q}), \qquad (24)$$

---

[6] Although for the properties of water there exist accurate models [22], here we want to use simplified relations, as these are more suited for automotive CPU usage.

where the limiting cases $c = 0$ and $c = 1$ require $h_y(0, T_{2,q}) = \overline{h}_y(1, T_{2,q}) = 0$ and $h_y(1, T_{2,q}) = \overline{h}_y(0, T_{2,q}) = 1$. For our purposes we write

$$h_y(c, T_{2,q}) = ce^{a_y(1-c)/T_{2,q}},\tag{25}$$

and

$$\overline{h}_y(c, T_{2,q}) = (1-c)e^{\overline{a}_y c/T_{2,q}},\tag{26}$$

with the coefficients a_y and $\overline{a}_y$, which have to be determined from experimental data or restrictions due to conservation laws.

A.1 Density

Generally, we approximate the temperature dependence of the density by means of a power series, where in the case of water, we restrict ourselves to quadratic order. For ethylene glycol, a linear approximation is sufficient for our purposes. From the conservation of mass, the density of the mixture within our approach is given by (c.f. Eqs. (25) and (26)) $a_y = \overline{a}_y = 0$, viz.

$$\varrho(c, T_{2,q}) = c\varrho_{C_2H_6O_2}(T_{2,q}) + (1 - c)\varrho_{H_2O}(T_{2,q}).\tag{27}$$

Here ϱ_X is the density of the component X. A comparison to experimental data reveals, that our model exhibits a maximum relative error of below 2.5 % in the temperature region between 250 and 390K[7].

A.2 Dynamic Viscosity

The dynamic viscosity η_X for the pure component X is described within a generalized phenomenological approach due to Raman [14, 15, 23] via

$$\eta_X = A_X e^{E_X(T_X)/(k_B T_X)},\tag{28}$$

where k_B gives the Boltzmann constant and T_X resembles the temperature of the pure component X. The coefficients $E_{X,0}$ and $E_{X,2}$ appearing in the energy functional $E_X(T_X) = E_{X,0} + E_{X,2}T_X^2$, and the prefactor A_X are determined from a fit to the data sheet.

For the interpolation, we observe, that a higher accuracy is achieved if we use the natural logarithm of the dynamic viscosity instead of setting $y = \eta$ in Eq. (24). Then determining the interpolation coefficients, we find $a_\eta, \overline{a}_\eta \ll T_{2,q}$, such that within the

---

[7] Given that the liquid phase exists for the considered volume concentration of ethylene glycol.

Eqs. (25) and (26) the exponential functions may be expanded to linear order. From this, we obtain

$$\eta\left(T_{2,q}\right) = \eta_{C_2H_6O_2}^{c(1+a_\eta(1-c)/T_{2,q})}\left(T_{2,q}\right)\eta_{H_2O}^{(1-c)(1+\overline{a}_\eta c/T_{2,q})}\left(T_{2,q}\right). \tag{29}$$

Comparing our model to experimental data, we find that in the aforementioned temperature region the maximum relative error is given by 1.8 %.

A.3 Specific Heat Capacity

The specific heat capacities of the pure components are given by means of the PPDS equation [15], where for the present purpose an approximation up to quadratic order terms in the reduced temperature $\tau_X = 1 - T_X/T_{X,crit}$ is sufficient, both for ethylene glycol and for water. Here $T_{X,crit}$ is given by the critical temperature of the component X.

As far as the interpolation is concerned, from the conservation of energy, we observe, that consistency requires to set $y = \varrho c_p$, with $a_{\varrho c_p} = \overline{a}_{\varrho c_p} = 0$. Thus we arrive at

$$c_p\left(c, T_{2,q}\right) = \frac{\varrho_{C_2H_6O_2}\left(T_{2,q}\right)}{\varrho\left(c, T_{2,q}\right)}c \ c_{p,C_2H_6O_2}\left(T_{2,q}\right) + \frac{\varrho_{H_2O}\left(T_{2,q}\right)}{\varrho\left(c, T_{2,q}\right)}\left(1-c\right) \ c_{p,H_2O}\left(T_{2,q}\right). \tag{30}$$

Utilizing this approach, we are able to model the specific heat capacity of the fluid within the fore cited temperature region and with a maximum relative error below 5.9 %.

A.4 Heat Conductivity

The heat conductivity λ_{H_2O} for water is described by means of a second order polynomial in temperature. For ethylene glycol a linear approximation is sufficient. For the interpolation function we set $y = \lambda$ and fit a_λ and $\overline{a}_\lambda$ to experimental data. The latter turn out to be in the same order of magnitude as temperatures relevant for our purposes, such that further simplifications by means of power series expansions cannot be put forward. Our model gives a satisfactory accuracy with a maximum relative error of below 6 %.

References

1. Zähr, J., Füssel, U., Ulrich, H.-J., Türpe, M., Ebert M., Weinbruch, S.: Anwendbarkeit von Benetzungsversuchen für verschiedene Metalle (Applicability of wetting trials for different metals). METALL **62**(10), 611 (2008)
2. Hawksworth, D.K., Sekulic, D.P., Yu, C.-N., Fu H., Westergard, R.G.J.: A mechanistic study of aluminium controlled atmosphere brazing processes. In: VTMS, p. 107 (2015)

3. Li, B., Akdogan, V., Li, Y., Yan, Y., Li, J., Wang, J.: A novel and efficient thermoelectric-generating (TEG) system of energy harvesting from exhaust gases of passenger vehicles. In: VTMS, p. 397 (2015)

4. Gotovskiy, M.A., Grinman, M.I., Formin, V.I., Aref'ev, V.K., Grigor'ev, A.A.: Use of combined steam-water and organic rankine cycles for achieving better efficiency of gas turbine units and internal combustion engines. Thermal Eng. **3**, 236 (2012)

5. Banzhaf, M., Hendrix, D., Schmidt, M.: Ecological advances in engine cooling. ATZ Worldwide **9**, 28 (2001)

6. Edwards, S., Müller, R., Feldhaus, G., Finkeldei, T., Neubauer, M.: The reduction of CO2 emissions from a turbocharged DI gasoline engine through optimised cooling system control. MTZ Worldwide **1**, 12 (2008)

7. Guhr, C., Zellbeck, H.: Turbocharging with low temperature charge air cooling and EGR. MTZ Worldwide **10**, 44 (2012)

8. Kadunic, S., Baar, R., Scherer, F., Zegenhagen, T., Ziegler, F.: Heat2Cool-Engine Operation at Charge Air Cooling below Ambient Temperature. 22. Aachen Colloquim (2013)

9. Wagner, J.R., Ghone, M., Dawson, D., Marotta, E.E.: Coolant Flow Control Strategies for Automotive Thermal Management Systems, SAE paper no. 2002-01-0713 (2002)

10. Wagner, J.R., Srinivasan, V., Dwason, D.M., Marotta, E.E.: Smart Thermostat and Coolant Pump Control for Engine Thermal Systems, SAE paper no. 2003-01-0272 (2003)

11. Setlur, P., Wagner, J.R., Dawson, D.M., Marotta, E.E.: An advanced engine thermal management system: nonlinear control and test. IEEE/ASME Trans. Mechatron. **10**(2), 210 (2005)

12. Salah, M.H., Mitchell, T.H., Wagner, J.R., Dawson, M.D.: Nonlinear-control strategy for advanced vehicle thermal-management systems. IEEE Trans. Veh. Tech. **57**(1), 127 (2008)

13. Khodabakhshian, M., Feng, L., Wikander, J.: Predictive control of the engine cooling system for fuel efficiency improvement. In: IEEE International Conference on Automation Science and Engineering (CASE), p. 61 (2014)

14. Herzog, A., Skorupa, F., Meinecke, R., Frase, R.: Thermal management in the air intake system of combustion engines. MTZ Worldwide **5**, 24 (2014)

15. VDI Heat Atlas, 2nd edn. p. 34 ff., Springer, Heidelberg (2010)

16. Roetzel, W., Spang, B.: Analytisches Verfahren zur thermischen Berechnung mehrgängiger Rohrbündelwärmeübertrager, Fortschr.-Ber. VDI, vol. 19(18). VDI-Verlag, Düsseldorf (1987)

17. Rötzel, W., Spang, B.: Thermal calculation of multipass shell and tube heat exchangers. Chem. Eng. Res. Des. **67**, 115 (1989)

18. Smith, D.M.: Mean temperature difference in cross flow. Engineering **138**(479), 606 (1934)

19. Pflaum, W., Mollenhauer, K.: Wärmeübergang in der Verbrennungskraftmaschine. Heat Transfer in the Combustion Engine. Springer, New York (1977)

20. Heuck, M.: Modellgestütztes Luftsystem-Management für einen Pkw-Dieselmotor mit Hoch- und Niederdruck-Abgasrückführsystemen, Dissertation (2009)

21. Landau, L., Lifshitz, E.M.: Fluid Mechanics. Course of Theoretical Physics, vol. 6, 3rd edn. Pergamon Press Ltd. (1966)

22. The International Association for the Properties of Water and Steam: Revised Release on the IAPWS Formulation 1995 for the Thermodynamic Properties of Ordinary Water Substance for General and Scientific Use (2014)

23. Raman, C.V.: A theory of the viscosity of liquids. Nature **111**, 532 (1923)